Front interaction on a ring electrode

Oleksiy Orlychenko, Yi Ye, and Hsueh-Chia Chang
Department of Chemical Engineering, University of Notre Dame, Notre Dame, Indiana 46556
(Received 2 December 1997)

Recent electrochemical experiments and simulations by Krischer and co-workers on a ring electrode reveal a unique transition mechanism for a bistable reduction reaction. The front boundaries of a localized pulse of higher potential are seen to accelerate around the ring to induce a very rapid transition. We show here that the accelerated transition is due to attractive front interaction across the pulse initially and around the ring in the final stage. Using coherent structure theory, we quantitatively correlate this interaction-induced acceleration to the dimensions of the electrodes. We also predict a critical width of the initial pulse below which the pulse will shrink and the transition is prevented. [S1063-651X(98)15305-9]

PACS number(s): 82.40.Ck, 47.54.+r, 82.45.+z

I. INTRODUCTION

The reduction rate of a negative ion at a working electrode has a nonmonotonic dependence on the electrode potential since an increase in potential can both repel the negative ion (hence decrease the reaction rate) and enhance the electron transfer rate [1]. When this reaction rate is balanced against the net current imposed by a constant potential drop across the electrodes, a bistable system can result with two stable homogeneous states—an active one with higher potential and a passive one. Due to the nonmonotonic dependence of the reaction rate on the potential in this bistable region and due to the lower potential drop across the electrolyte, the ''active'' state with a higher potential actually yields a lower current across the electrode.

If a few layers of water molecules are packed against the electrodes, as is commonly believed to be the case near the electrodes, some electrons and ions are spent charging the resulting ''double-layer'' capacitor instead of undergoing the electron-transfer reduction reaction. The two processes are often modeled as a capacitor in parallel with a non-Ohmic resistor representing the reaction. Due to the large capacitance of this molecular-level double layer, its charging dynamics is often slow and observable compared to the time scale for ion transport to and across the double layer and electron transfer during the reduction reaction. In fact, this slow dynamics has been shown to be coupled with the bistable kinetics to yield nontrivial dynamics such as hysteresis and excitability, as well as complex nonlinear dynamics near high-order dynamic singularities like Takens-Bogdanov [2]. If, in addition, a reference electrode can be placed sufficiently close to the working electrode, spatial gradient in the potential can be introduced in the tangential direction along the electrode. The spatial gradient is introduced by the finite and constant conductivity in the neutral electrolyte between the electrodes and the potential there satisfies the three-dimensional Laplace equation. The reaction, on the other hand, occurs on the working electrode surface only. Nevertheless, one expects that, in the limit when the electrode separation vanishes, the bistable kinetics can couple with the bulk potential gradient to introduce complex spatiotemporal patterns on the electrode, as in other reaction-diffusion systems with similar kinetics. Indeed, fronts reminiscent of bistable reaction-diffusion systems are found in a series of experiments and simulations carried out by Krischer and her co-workers [3,4].

Krischer's working electrode is an Ag ring electrode for the reduction of $S_2O_8^{2-}$. The width of the ring electrode is much smaller than the circumference L and the separation from the reference electrode w. Consequently, both the radial variation across the width and the ring curvature can be omitted such that the potential on the electrode is pseudo-one-dimensional. The electrode is originally in the passive homogeneous state and a localized pulse of higher potential is then introduced by a microprobe. The boundaries of the pulse are observed to evolve into fronts separating the active region within the pulse from the passive surrounding. The fronts then expand until they meet on the other side of the ring such that the entire electrode is in the active state.

It is in the propagation of these fronts where front dynamics different from one-dimensional diffusion-reaction fronts are observed by Kirscher's group. As seen in their simulations [4] shown in Figs. 1 and 2, when (w/L) is small, the fronts propagate at constant speed around the ring as the active state replaces the passive one. The total current is also seen to drop linearly in time as seen in Fig. 2, reflecting the constancy of the speeds of the fronts. This is the expected behavior for the front of a one-dimensional bistable reaction-diffusion system. However, when the reference electrode is moved further away, such that (w/L) is of unit order or larger, the front and the current evolution clearly shows nonlinear behavior in Figs. 1 and 2. The fronts seem to accelerate across the ring such that the active state replaces the passive one in a rapid transition. Moreover, as shown in Fig. 1(d), when (w/L) is much larger than unity, the pulse actually extinguishes as its fronts collapse into each other instead of expanding. The subsequent homogeneous ''ignition'' to the active state is because the simulation was done under conditions of a single active state (excitable) system instead of a true bistable system. Nevertheless, the extinction of the initial pulse is unmistakable and would also have occurred in a bistable system.

Accelerated fronts and extinction of a pulse are typically associated with a two-dimensional reaction-diffusion system whose spatiotemporal dynamics is far richer than the one-dimensional case [5]. That the same phenomena can appear

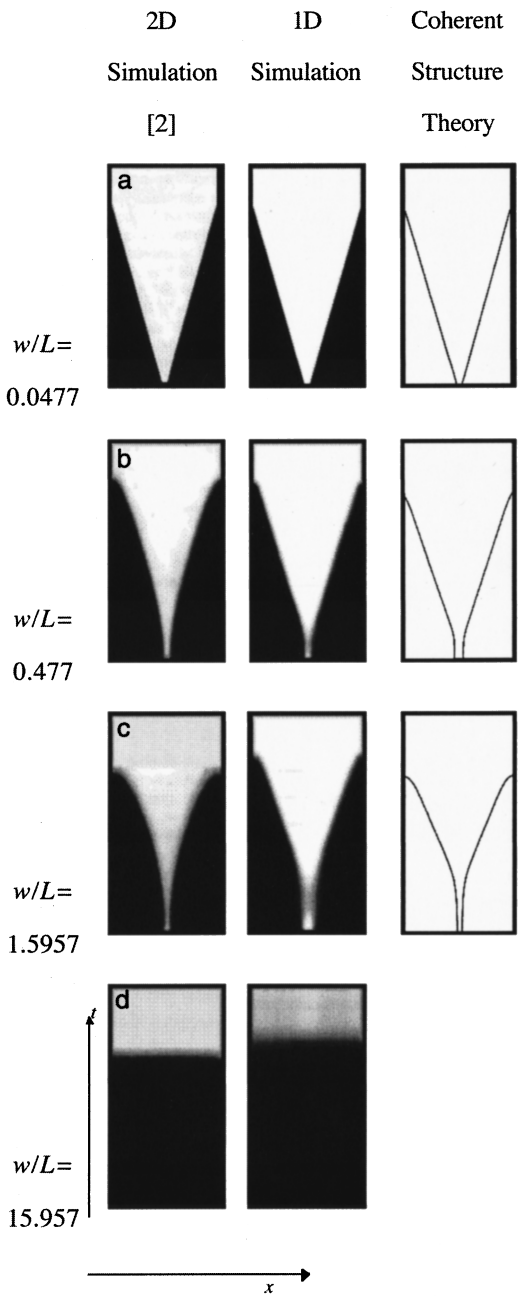

FIG. 1. Comparison of the 2D and 1D theories: 2D simulation [2], 1D simulation. Coherent structure theory: the front evolution.

in a pseudo-one-dimensional system hence suggests that other complex dynamics are possible on the ring electrode.

The curious accelerated front dynamics has been attributed to the ''global coupling'' effect representing higher coupling between different points on the ring electrode as the electrode separation increases [4]. The argument is that the increased gap distorts equipotential lines between the electrodes from a linear topology in a thin gap to fully curved ones in a wide one. As a result, the potential gradient along the ring is amplified in the latter case which, in turn, enhances the flux of the higher potential to the lower-potential passive region via the bulk electrolyte. In the limit of $(w/L)\ll 1$, the flux through the electrolyte has been shown to produce a net diffusive flux along the electrode [4]. It can hence be modeled as a pseudo-one-dimensional reaction-

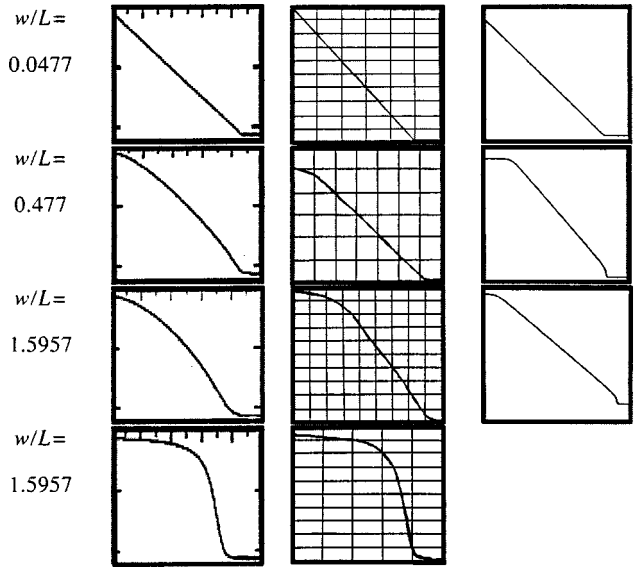

FIG. 2. Comparison of the 2D and 1D theories: 2D simulation [2], 1D simulation. Coherent structure theory: the total current vs time.

diffusion equation. It was believed that enhanced flux in the limit $(w/L)\gg 1$ cannot be modeled as one-dimensional diffusion and hence the accelerated fronts are a two-dimensional effect.

We show here that both the accelerated front and pulse extinction phenomena can still exist for a one-dimensional diffusion-reaction system in a periodic domain like the ring electrode. As a result, while nontrivial dynamics are still possible, they are not as rich as a truly two-dimensional one. Both phenomena are due to long-range interaction of the two fronts through the bulk electrolyte, which can often be modeled as one-dimensional diffusive coupling even for (w/L) of unit order. The accelerated front phenomenon is due both to initial interaction across the pulse when it is narrow and final-stage interaction around the ring when the pulse is wide. The extinction phenomenon, however, is only due to the former interaction.

II. EFFECTIVE ONE-DIMENSIONAL DIFFUSION COEFFICIENT

We begin by neglecting the potential variation in r, the ring curvature, and the finite circumference of the ring. The electrolyte between the electrodes is confined to an infinite strip with boundary conditions $\phi=0$ at the reference electrode at the plane $z=w$ and $\phi=V-u(x)$ at the plane $z=0$ corresponding to the outside surface of the double layer on the working electrode. The total applied voltage is V and $u(x)$ is the potential drop at the double layer. The potential within the strip is governed by the two-dimensional Laplace equation and we hence use the conformal map $(\xi,\eta)=(e^{\pi x/w}\cos \pi z/w, e^{\pi x/w}\sin \pi z/w)$ to map the strip into the half-plane $\eta>0$ with boundary conditions $\phi=0$ for $\xi<0$ and $\phi=V-u(x)$ for $\xi>0$ at the boundary $\eta=0$. Using the Poisson formula, one gets

$$\frac{\partial \phi}{\partial z}(x,z)=\int_{-\infty}^{+\infty} G(p,z)[V-u(x+p)]dp$$

or, breaking the integral by taking into account the periodicity of $u(x)$, as

$$\frac{\partial \phi}{\partial z}(x,z)=\sum_{k=-\infty}^{k=+\infty}\int_{-L/2}^{+L/2} G(p+kL,z)[V-u(x+p)]dp, \tag{1}$$

where k is a integer and the Green's function is

$$G(p,z)=\frac{1}{\pi}\frac{e^{\pi p/w}[\tan^2\ \pi z/w-(1-e^{\pi p/w})^2]}{\cos^2\ \pi z/w[\tan^2\ \pi z/w+(1-e^{\pi p/w})^2]^2}, \tag{2}$$

which is singular as both p and z approach zero, $G(p,z)\rightarrow -p^{-2}$ as $z\rightarrow 0$. This sharp singularity at $p=0$ allows us to estimate the flux at the electrode, which is directly proportional to $\partial\phi/\partial z$ at $z=0$, by expanding the kernel in convolution (1). We hence expand about $p=0$

$$u(x+p)=u(x)+\frac{du}{dx}\,p+\frac{1}{2}\frac{d^2u}{dx^2}\,p^2+K \tag{3}$$

and assume that $u(x)$ is sufficiently smooth such that its derivatives become successively smaller and the expansion converges near $p=0$. From contour integration, we can find the first few moments of the kernel [for the case $(w/L)\rightarrow 0$, when only the term with $k=0$ survives]:

$$\lim_{z\rightarrow 0}\int_{-\infty}^{+\infty} G(p,z)dp=-1/w,\quad \lim_{z\rightarrow 0}\int_{-\infty}^{+\infty} pG(p,z)dp=0,$$

$$\lim_{z\rightarrow 0}\int_{-\infty}^{+\infty} p^2G(p,z)dp=-\frac{2w}{3}.$$

As a result, provided the spatial gradient of u is not excessively sharp, the surface flux in the original unscaled coordinate system can be approximated by [for the case when $(w/L)\rightarrow 0$]

$$\left.\frac{\partial\phi}{\partial z}\right|_{z=0}=-\frac{V-u(x)}{w}-D_\infty\frac{d^2u}{dx^2}, \tag{4}$$

where the ''effective diffusivity'' in units of length is given by $D_\infty=w/3$, the ''long-wave limit'' obtained by Mazouz and Krischer [4].

This effective one-dimensional diffusivity applies whenever the domain of p is sufficiently large and $u(x)$ is sufficiently smooth. The latter is trivially satisfied except during the initial transients when the imposed pulse has step-function boundaries. The former is valid only if the circumference is sufficiently large compared to w. To estimate how finite circumference distorts our diffusivity, we again retain the term with $k=0$ in Eq. (1) to obtain

$$D=D_\infty\left(\lim_{z\rightarrow 0}\int_{-L/2}^{+L/2} p^2G(p,z)dp\ \Big/\ \lim_{z\rightarrow 0}\int_{-\infty}^{+\infty} p^2G(p,z)dp\right) \tag{5}$$

and find that D only deviates significantly from D_∞ if (w/L) is in excess of unity. All $k\neq 0$ terms are exponentially small because of the $\exp[-|p|]$ dependence of the Green's function (2) at $\pm\infty$. Hence, only the corrected $k=0$ term needs to be included. The one-dimensional approximation (4) hence remains valid [when corrected diffusion coefficient (5) is used] even for (w/L) close to unity where the simulation of Mazous and Krischer in Figs. 1(b) and 1(c) clearly show front acceleration. This phenomenon should hence be capturable with a one-dimensional diffusion-reaction equation. Our estimate of D/D_∞ from Eq. (4) yields 1.0, 0.99, 0.55, and 0.29 for $(w/L)=0.0477$, 0.477, 1.5957, and 15.957 of Fig. 1. The validity of long-wave expansion even for (w/L) of unit order is due to the strong p^{-2} singularity at $p=0$ when z tends to zero. This renders Eq. (3) as a converging series even for $u(x)$ with relatively high gradients. Moreover, the diffusivity actually decreases as one fixes w and decreases L (increase w/L), which is inconsistent with the speculation that global coupling increases with decreasing L.

III. ONE-DIMENSIONAL REACTION-DIFFUSION EQUATION

To scrutinize the accelerating front phenomenon more closely, we include Eq. (4) with the general diffusivity of Eq. (5) in a charge balance across the parallel circuit of the non-Ohmic reaction resistor and the double-layer capacitance,

$$Cu_t=-r(u)+\sigma'\phi_z(z=0),$$

where σ' is a conductivity in the bulk electrolyte and C is the double-layer capacitance. The following transformations: $(x,z)\rightarrow(Lx/2\pi,wz)$, $t\rightarrow(CRT/nF)r_0t$, $u\rightarrow(RT/nF)u$, $V\rightarrow(RT/nF)V$, $\sigma\rightarrow(RT/r_0nF)\sigma'$, and $i=r/(r_0nF)$ yield

$$u_t=-i(u)+(\sigma/w)[V-u+Du_{xx}] \tag{6}$$

where r_0 is a typical reaction rate, n is the charge number of the ion, F is the Faraday constant, and $D=Dw(2\pi/L)$.

The dependence of the $S_2O_8^{2-}$ reduction reaction on the potential has been fitted empirically [4] to yield a reaction current of $i=0.0365u^3+17.23u^2+2019.6u$. The reported value of the third coefficient 2019.6 by Mazouz and Krischer is actually 2039.6 but such a coefficient yields an excitable system instead of bistability and we have altered it to 2019.6 here. The initial pulse width for simulation is always fixed at 0.2 in the scaled x coordinate in Eq. (6). In the simulations of Mazouz and Krischer of the full two-dimensional problem shown in Fig. 1 and 2, σ/w and V are held constant at 10 and -350, respectively. We have simulated Eq. (6) with the same coefficients and, as shown in the Figs. 1 and 2, have obtained front profiles and current evolution curves that are quantitatively consistent with the two-dimensional simulation. The only error arises during the initial phase when the pulse has a large gradient. Our estimated diffusivities D are probably too low during this interval. Fortunately, this transient for front formation is rather rapid and does not affect the later front acceleration dynamics.

Since σ/w is constant during these simulations, we note that this does not correspond to real experimental conditions where w is varied and, therefore, σ/w cannot be constant. If one envisions a fictional experiment where the ring circumference L is varied while w is constant, then the simulations in Fig. 1 correspond to a different initial width with Fig. 1(a) having a larger width. This suggests that the acceleration is

not present in that figure not because the diffusivity is small (it is, in fact, the largest possible) but because the initial width is too large for front interaction to take place. In the actual experiment when L is fixed and w is varied, the bistable system yields an excitable system with a unique homogeneous state at large w/L and the evolution should resemble Fig. 1(d). However, for intermediate values of w/L, the degree of front acceleration is determined not by global coupling but by the width of the reaction front relative to the initial and the final front separation. The front width is then a complex function of w/L and it is not clear that acceleration always increases with w/L.

To demonstrate this, we rewrite Eq. (6) as a one-parameter diffusion-reaction system

$$u_\tau = u_{\xi\xi} - u(u-1)(u+\alpha), \tag{7}$$

where $\tau = ta(s_1-s_2)^2$, $\xi = x(a(s_2-s_1)/D)^{1/2}$, and $a=0.0365$. For the standard conditions in Fig. 1, $s_i = (-257.83,-212.47,-1.75)$ are the three roots of the polynomial $i(u)+(\sigma/w)(V-u)$. Hence, the key parameter α is $(s_3-s_2)/(s_2-s_1)=4.645$ for the specified conditions. The circumference is now of length $2\pi(a(s_2-s_1)/D)^{1/2}$. Since all the conditions in Fig. 1 correspond to the same value of α, the only change is in the circumference length. Front interaction is hence expected whenever the front width, which has been scaled to unity here, is smaller than $2\pi(a(s_2-s_1)/D)^{1/2}$. For w/L less than unity, this corresponds to $0.74(L/w)>1$, which is always satisfied. Even at $w/L=1.5957$ of case c, the condition is just barely violated and one may still be able to describe the acceleration rate through front interaction.

IV. REACTION FRONT AND SPECTRUM

The two front solution to Eq. (7) can be readily obtained by inspection,

$$u_\pm = \tfrac{1}{2}\{1-\alpha \pm (1+\alpha)\tanh[(1+\alpha)(\xi - c_\pm \tau)/2\sqrt{2}]\}, \tag{8}$$

with speed $c_\pm = \pm(\alpha-1)/\sqrt{2}$.

Transforming Eq. (7) into a moving coordinate with the speed c_* of a particular front u_* and linearizing about that front, one obtains the disturbance equation $\partial\nu/\partial\tau = L\nu$, where $L=\partial^2/\partial\xi^2 + c_*\partial/\partial\xi - e$ and $e=3u_*^2+2(\alpha-1)u_* - \alpha$. Perturbation about the constant-speed front, such as the observed acceleration, is determined by the spectrum of L. This spectrum contains both discrete and essential spectra [5] the corresponding eigenfunctions of which approach zero and bounded oscillations, respectively, at the two infinities. Judging from the simulations, the front is stable and both spectra lie in the left half of the complex plane. There is, however, a neutral mode that arises from the translational symmetry—Eq. (7) in the moving coordinate is invariant to $\xi \to \xi + \xi_0$ and translations of the fronts (8) are still front solutions. A simple differentiation of Eq. (7) in the moving frame shows that $L\,(du_*/d\xi)=0$ and the eigenfunction of this discrete neutral mode is $du_*/d\xi$.

The adjoint eigenvalue problem defined by $L^+ = \partial^2/\partial\xi^2 - c_*\partial/\partial\xi - e$ also has a neutral discrete mode with eigenfunction φ_*. Hence, if we expand the disturbance of w in $du_*/d\xi$, the coefficient of expansion is (w,φ_*) if φ_* is normalized such that $(\varphi_*, du_*/d\xi)=1$ and the inner product is defined as $(f,g)=\int fg\,d\xi$ in the moving frame. Using a shooting scheme described in [6], we have constructed the adjoint eigenfunction φ_*. For the standard conditions of $\alpha=4.645$, the computed neutral eigenfunctions are shown in Fig. 3. The most pertinent parts of this eigenfunction are its decay rates toward the active and passive parts of the front. Using the forward-stepping front (u_-) located at $\xi=0$ as a reference, these can be represented as

$$\lim_{\xi\to+\infty} \varphi_- = \delta_+ e^{-\sqrt{2}\alpha\xi}, \qquad \lim_{\xi\to-\infty} \varphi_- = \delta_- e^{\sqrt{2}\xi}.$$

Due to obvious symmetries between $u_\pm$, the adjoint eigenfunction for u_+ would simply be the mirror image of u_-. We depict our computed δ ($\delta_+ = \delta_- = -\delta$ within numerical accuracy) in Fig. 4.

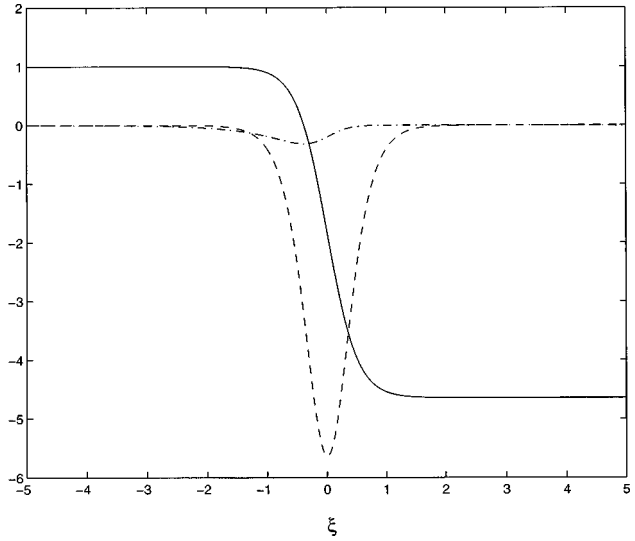

FIG. 3. Solid line, foward stepping front u_-; dashed line, neutral mode $du_-/d\xi$; dash-dot line, adjoint eigenfunction φ_-.

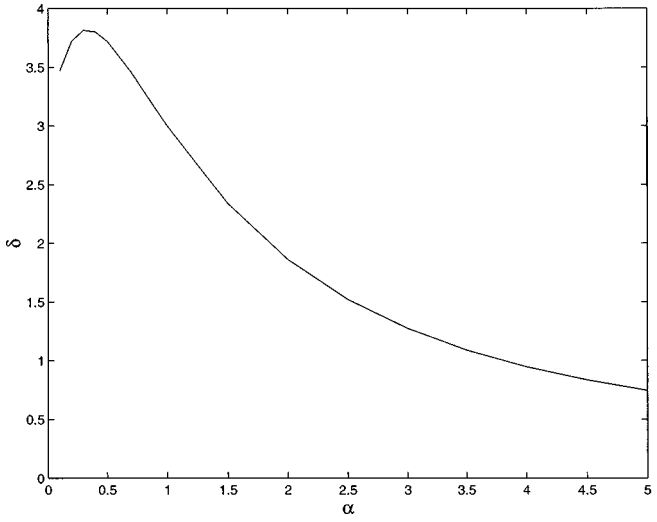

FIG. 4. Dependence of front interaction parameter δ on the system parameter α.

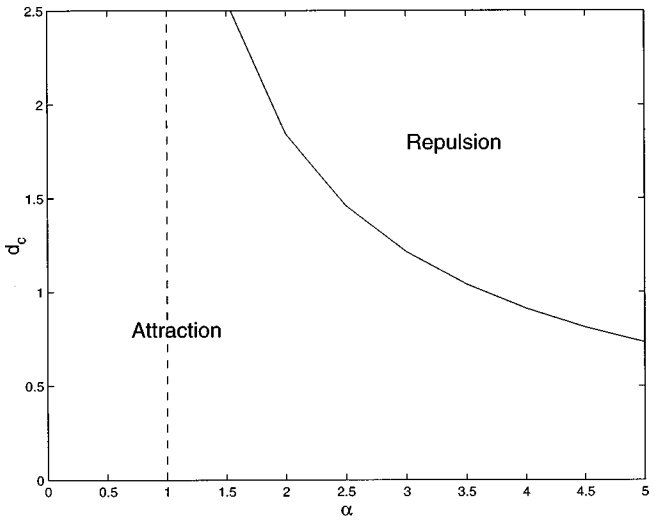

FIG. 5. Dependence of critical distance d_c on the parameter of system α.

V. COHERENT STRUCTURE THEORY

Since the dominant neutral mode corresponds to a translation, when two fronts are placed sufficiently close that they feel the presence of each other and not too close to destroy the front structure, the resulting interaction would cause both fronts to translate. Consider the initial interaction immediately after the fronts are established, we seek the interaction force on each front at any given moment in time. Let the left front u_- be located at $\xi=0$ at this moment. Any interaction would translate this front to a new position $\xi_-(t)$ and the translation is simply $u_-(\xi-\xi_-(t))$. An expansion for small $\xi_-(t)$ yields $u_-\sim u_-(\xi)-\xi_-(t)du_-/d\xi$ and we see the coefficient of the neutral eigenfunction has a simple physical interpretation—the position of the front. Similarly, the right front situated at the distance d to the right of u_- can be written as $u_+\sim u_+(\xi)-\xi_+(t)du_+/d\xi$.

At any instance in time, the entire pulse can be written as

$$u\sim u_-(\xi-\xi_-(t))+u_+(\xi-\xi_+(t))+\alpha.$$

Upon substituting this expression into Eq. (6), one obtains

$$-\dot{\xi}_+u'_+(\xi-\xi_+)-\dot{\xi}_-u'_-(\xi-\xi_-) =c_+[u'_-(\xi-\xi_-)-u'_+(\xi-\xi_+)]-f_1,$$

where

$$f_1(\xi)=[u_+(\xi-\xi_+)+\alpha][u_-(\xi-\xi_-)+\alpha][3u_+(\xi-\xi_-) +3u_-(\xi-\xi_-)-2\alpha-2].$$

Taking inner product with respect to the adjoint $\varphi_\pm$ to isolate each front, one obtains two equations for $\dot{\xi}_+$ and $\dot{\xi}_-$. Subtracting the two equations, a single evolution equation for d results:

$$\dot{d}=g_1(d,\alpha)=\dot{\xi}_+-\dot{\xi}_-=2c_+-\frac{2(f_1,\varphi_-)}{1-[u'_+(\xi-d),\varphi_-]}. \tag{9}$$

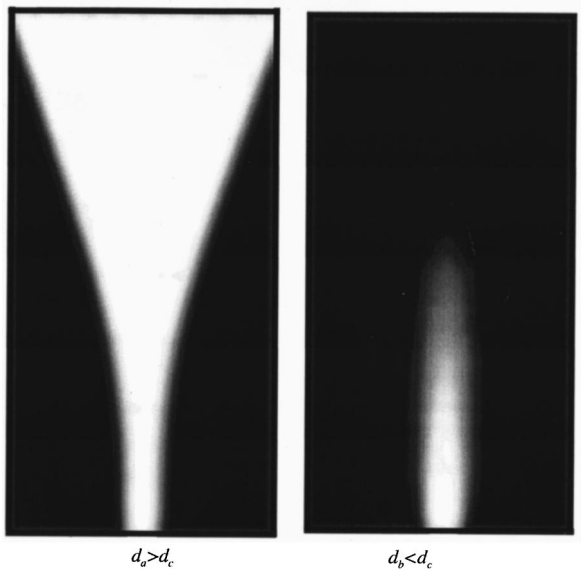

FIG. 6. 1D numerical simulations for the case $\alpha=4.5645$, $d_a=1.01d_c$, and $d_b=0.99d_c$ ($d_c=0.83$).

For long-range interaction, the intervals for inner products involve overlapping exponential terms of the form

$$u_+(\xi)\sim-\alpha+(1+\alpha)\exp\{-(1+\alpha)\xi/\sqrt{2}\},$$

$$u_-(\xi)\sim-\alpha+(1+\alpha)\exp\{-(1+\alpha)(d-\xi)/\sqrt{2}\},\quad\text{and}\quad f\sim -(2+8\alpha)(1+\alpha)^2\exp\{-(1+\alpha)d/\sqrt{2}\}.$$

One then obtains

$$\dot{d}\sim 2c_+-(4\delta/\sqrt{2\alpha})(1+4\alpha)(1+\alpha)^2e^{-(1+\alpha)d/\sqrt{2}} \tag{10}$$

for $d\gg 1$.

The constant term $2c_+$ corresponds to two noninteracting fronts that propagate in opposite direction while the exponentially decaying second term represents the initial attractive interaction between the two fronts. Front acceleration is actually due to an attractive front interaction that prevents the fronts from moving at their normal speeds.

At the end of the translation when the pulse width approaches the ring circumference, the fronts interact now on the other side and a similar analysis yields

$$\dot{d}\sim 2c_+-(4\delta/\sqrt{2})(4+\alpha)(1+\alpha)^2e^{-(1+\alpha)(L-d)/\sqrt{2}}, \tag{11}$$

where L is the rescaled circumference of the ring. The interaction is again attractive but now the fronts accelerate toward each other, instead of being bound during the initial attractive interaction.

VI. INTERACTION DYNAMICS AND CRITICAL PULSE WIDTH

In Figs. 1 and 2 we compare the front acceleration dynamics predicted by Eqs. (10) and (11) to those from the initial two-dimensional simulations of Mazouz and Krisher and one-dimensional simulation using Eq. (6). Except for case d when the front width is much larger then the circum-

ference and hence the fronts are never established, the simple coherent structure theory yields excellent agreement. There is almost no interaction for case a, the initial and final interactions governed by Eqs. (10) and (11), respectively, are clearly evident in case b while they tend to overlap in case c. The theory also predicts the critical width d_c for the initial pulse defined by $g_1(d_c,\alpha)=0$ shown in Fig. 5. Pulses with initial widths smaller than d_c would extinguish instead of expanding. This is clearly corroborated by the one-dimensional simulation shown in Fig. 6.

Although the accelerated front dynamics and extinction phenomena are shown to be driven mostly by one-dimensional front interaction, its dynamics can still be very rich if there are multiple pulses [7] and if the exponential tails can be made to oscillate [6]. While their spatiotemporal dynamics are not as rich as truly two-dimensional problems, the statistics of multifront coalescence has been studied theoretically [7] and ring electrode experiments can corroborate theoretical predictions.

ACKNOWLEDGMENTS

This work was supported by NSF Grant NOS. CTS95-22277 and ECS97-06873. We are grateful to K. Krischer for bringing this problem to our attention and for her input.

[1] A. Frumkin, Z. Elektrochem. **59**, 807 (1955).
[2] W. Wolf, J. Ye, M. Purgand, M. Eiswirth, and K. Doblhofer, Ber. Bunsenges. Phys. Chem. **96**, 1797 (1992).
[3] G. Flatgen and K. Krischer, Phys. Rev. E **51**, 3997 (1995); G. Flatgen and K. Krischer, J. Chem. Phys. **103(13)**, 5428 (1995); G. Flatgen, K. Krischer, and B. Pettihger, Science **269**, 668 (1995); N. Mazouz, K. Krischer, G. Flatgen, and G. Ertl, J. Phys. Chem. B **101**, 2403 (1997).
[4] N. Mazouz and K. Krischer, Phys. Rev. E **55**, 2260 (1996).
[5] C. P. Schenk, M. Or-Guil, M. Bode, and H-G. Purwins, Phys. Rev. Lett. **78**, 3781 (1997).
[6] H.-C. Chang, E. A. Demekhin, and D. I. Kopelevich, Physica D **97**, 353 (1996); H.-C. Chang and E. A. Demekhin, in *Structure and Dynamics of Nonlinear Waves in Fluids*, edited by A. Mieke and K. Kirchgassner (World Scientific, Singapore, 1995), pp. 24–41.
[7] J. Rubinstein, P. Sternberg, and J. B. Keller, SIAM (Soc. Ind. Appl. Math.) J. Appl. Math. **53**, 1169 (1993); K. Kawasaki and T. Otha, Physica A **116**, 273 (1982).